Research Article

Kangsheng Xu* and Ying Li

The violent ground motion before the Jiuzhaigou earthquake Ms7.0

https://doi.org/10.1515/geo-2020-0184
received November 06, 2019; accepted July 23, 2020

Abstract: An Ms7.0 earthquake occurred in Jiuzhaigou, Sichuan Province, China, on August 8, 2017. In this study, we used the vertical component data from 31 seismic stations near the epicenter from May 1 to August 20, 2017, to calculate the amplitude spectrum hourly using the fast Fourier transform method. Furthermore, the spectral area of the low frequency band (0.02–1 Hz), which represents the energy of low frequency motion, was calculated. In this way, the temporal and spatial variations in the vertical ground motion in this region were determined. Four high-value processes occurred in mid-June, mid-July, late July, and early August (the last three are discussed in this article). Based on a comparison with the local meteorological data, the meteorological factors had no influence, local geological factors did not affect the results, and typhoon factors did not show obvious correlation. Combined with the results of previous studies, we believe that the increase in the spectral area reflects the intense movement of deep material in the region related to the Jiuzhaigou earthquake. The spatial distribution of the spectral area (energy) reveals that the deep material moved eastward rapidly, was obstructed by the Sichuan Basin, and expanded to the northwest in a U-shaped channel, which may be the main dynamic factor for the formation or triggering of the earthquake.

Keywords: Ms7.0 Jiuzhaigou earthquake, ground motion, FFT, amplitude spectrum, spectral area, dynamic process

1 Introduction

On August 8, 2017, at 21:49:24, an Ms7.0 earthquake (33.14°N, 103.79°E) occurred in Jiuzhaigou County, Sichuan Province, China, with a focal depth of 20 km (http://news.ceic.ac.cn/CC201808211947.html). The earthquake was located in the northeastern margin of the Bayan Hara block, which is surrounded by the eastern segment of the East Kunlun Fault, the Longriba Fault, the Minjiang Fault, the Huya Fault, and the Tazang Fault. The northern segment of the Huya Fault is a left-lateral strike-slip fault, and the southern segment is a thrust fault. To the east of this fault is the Longmenshan Fault, which trends northeast. The Longmenshan Fault is a thrust fault between the Bayan Hara block and the Sichuan Basin (Figure 1). A more consistent view is that the seismogenic fault of the earthquake is in the extension line of the northern segment of the Huya Fault [1,2]. Several studies have been published on this earthquake. Based on the distribution of the aftershocks, the orientation of the long axis of the intensity determined from the field investigation, and the investigation of the collapses and landslides caused by the earthquake, several studies have pointed out that the seismogenic fault of this earthquake should be the northward extension of the Huya Fault, which is a left-lateral strike-slip fault, and the fracture process occurred upward from depth [1–3]. Based on the seismic observation data, several scholars have studied the crustal structure in this region. The results show that there are low velocity layers in the middle crust at a depth of 20–40 km throughout most of the regions and a few in the upper crust at depths of 10–20 km and in the lower crust at depths of 40–60 km [4]. On the southern side of the Bayan Hara block, the southeastward middle-lower crustal flow was obstructed and turned southward in the Luding-Shimian area. On the northern side of the Bayan Hara block, it flows northeastward, and there is a southeastward crustal flow perpendicular to the Longmenshan Fault. This study also shows that the crustal flow in the middle and lower crust is also diverted into the upward and downward branches after being obstructed by the Sichuan Basin, and then, it intrudes into the upper crust [5]. As for the dynamic background of the earthquake, it is generally believed

* **Corresponding author: Kangsheng Xu,** Gansu Seismic Network, Lanzhou Institute of Seismology, China Earthquake Administration, Lanzhou, China, e-mail: xuks@foxmail.com
Ying Li: Earthquake Emergency Center, Lanzhou Institute of Seismology, China Earthquake Administration, Lanzhou, China

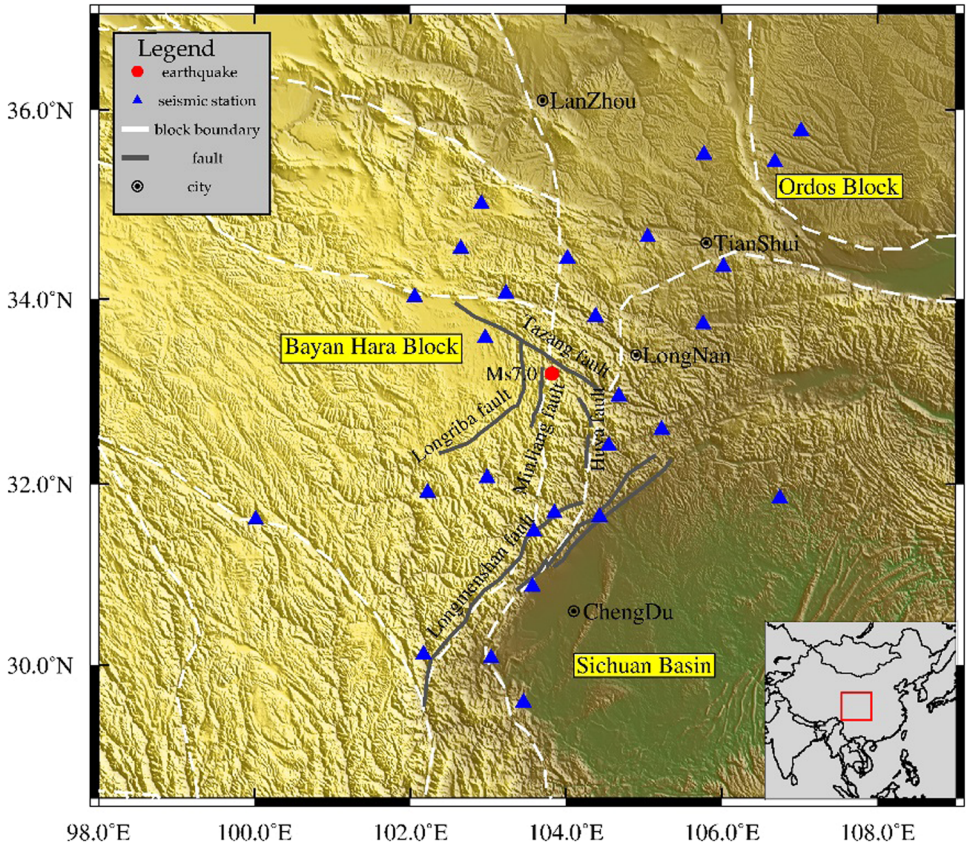

Figure 1: The distribution of the seismic stations used in this study and location of the Jiuzhaigou earthquake (Ms7.0).

that the eastward movement of the Bayan Hara block was strongly obstructed by the Sichuan Basin, which caused the accumulation of energy and led to formation of the earthquake [1–4]. Several studies have concluded that the earthquake was the result of the northeastern extrusion of the lower crust in the northeastern part of the Bayan Hara block [6,7], but a more detailed dynamic process has not been reported. In this article, the temporal and spatial characteristics of the crustal movement in this region are studied in detail using seismic observation data collected before the earthquake, and the relationship between the characteristics of the crustal movement in this region and the formation and occurrence of the Jiuzhaigou earthquake is discussed accordingly.

2 Methods

Our research period is from May 1 to August 20, 2017. The data were collected from 13 stations in the Gansu Seismic Network and 18 stations in the Sichuan Seismic Network, China. All of the stations have broadband seismographs with a frequency range of 60 s to 50 Hz. These stations are mainly distributed around the epicenter (Figure 1).

The signal recorded by a seismograph contains abundant frequency components. When a finite signal is expressed in the frequency domain, the signal energy is distributed at all of the frequency points, and the amplitude spectrum represents the signal energy at each frequency point. Generally, the high-frequency band of seismic records describes the shallower, small-scale, medium motion state, whereas the low-frequency band carries more deep, large-scale motion information. Since the bandwidth of the seismograph is 60 s to 50 Hz, and we focused on the low-frequency motion, the frequency range used in this study was 0.02–1 Hz. Herein, we used the spectral area (the area of the geometric shape formed by the spectral curve and the transverse axis) of this frequency band to represent the energy of the low-frequency ground motion (Figure 2). The trial calculation shows that this method reduces the sensitivity of the accidental vibration interference to the peak amplitude and makes the result more robust than the conventional peak spectrum method.

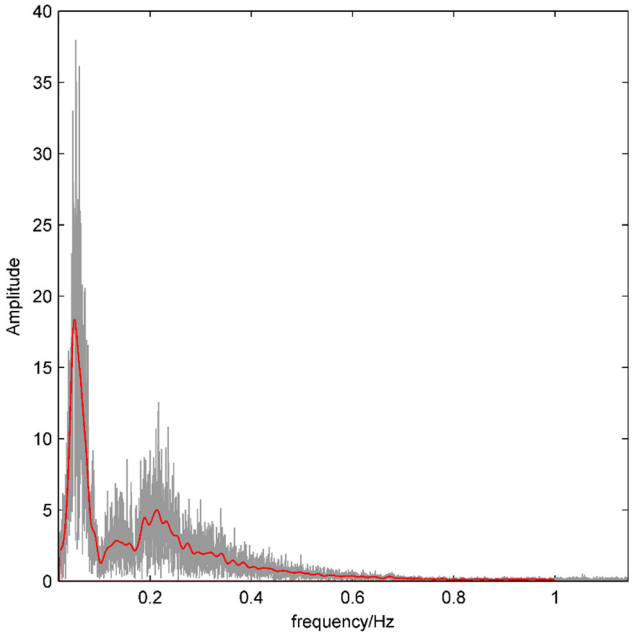

Figure 2: The amplitude spectrum of the ground motion.

The data processing steps are as follows.

1. The seismic observation records of 31 stations (112 days) were collected as the data for the study.
2. The fast Fourier transform (FFT) of the hourly vertical recording was calculated and the amplitude spectrum was obtained.
3. The amplitude spectrum was smoothed. The 0.02–1 Hz spectral curve and the transverse axis form a geometric shape (area enclosed by the red line in Figure 2). The area of this shape was calculated. This is defined as the spectral area.
4. For each station, 2,688 spectral area values were obtained. The time series curve of the spectral area values from the 31 stations is shown in Figure 3.

3 Results

From May 1 to August 20, 2017, the temporal variation in the spectral areas for the 31 stations is shown in Figure 3, in which the black thick line is the mean line for all of the stations. During the study period, there were four high-value processes, which occurred in mid-June, mid-July, late July, and early August. Since the last three high-

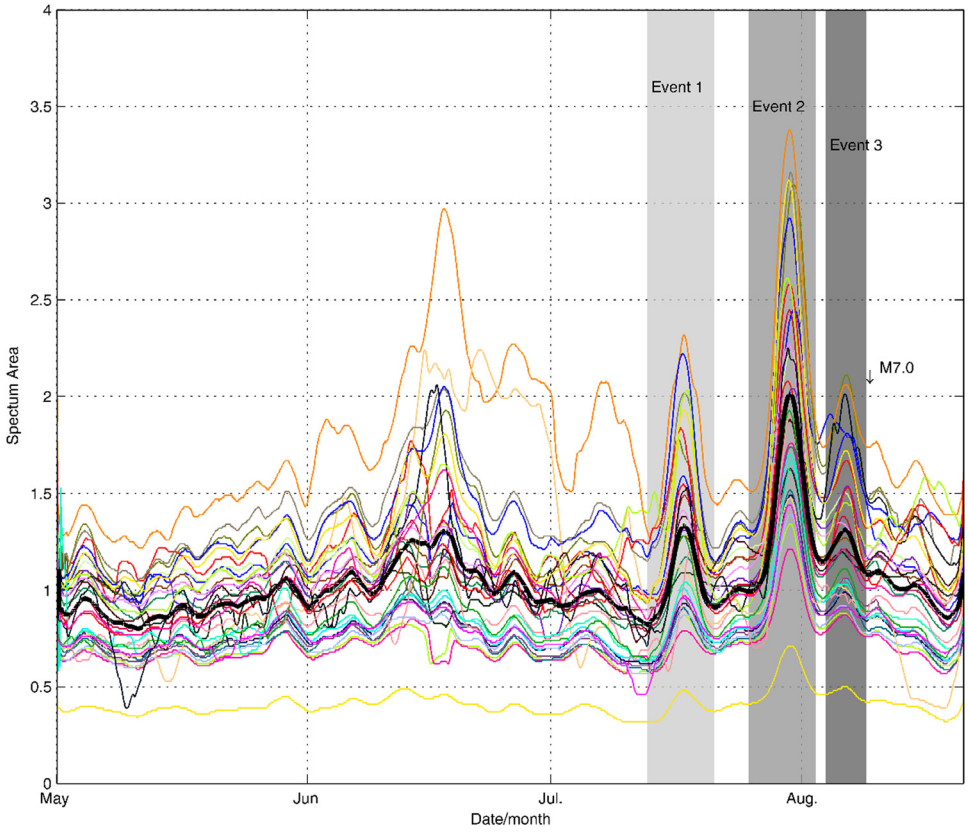

Figure 3: The temporal variation in the spectral areas (May 1–August 20, 2017). The black thick line is the mean value of all of the stations.

value processes have a good consistency, this study focuses on the latter three processes, which are called event 1 (July 11–21), event 2 (July 25–August 2), and event 3 (August 3–7) in chronological order. Event 2 has the largest amplitude, followed by event 1, and event 3 has the smallest amplitude. In the following description, the high value of the spectrum area is abbreviated as the high value, and its distribution area as the high value area.

To discuss the spatial characteristics of the three events, the mean values of each station from May 16 to May 31 were taken as reference values (or normal values). Their spatial distribution is shown in Figure 4a. The areas with slightly higher values mainly occurred on the western margin of the Sichuan Basin. There is a strip between Songpan-Heishui and Bazhong (about 1–2), and the rest are all below 0.8. Figure 4b shows the spatial distribution of event 1. The high value distribution range is similar to that in Figure 4a, but the values are larger, about 1.5–2.3, and the value of the low value area is larger, about 0.7–1.0. The highest value area is near Emeishan, which extends northeastward along the edge of the Sichuan Basin, and is connected to the Songpan-Heishui region. Figure 4c shows the spatial distribution of event 2, which is the largest event. The value in the study area increases overall. The peak area appears in the northwestern part of Emeishan, with values of 3–3.6. The high value area extends to the northeast along the edge of the Sichuan Basin, with values of 2.6–3.0. The value of the high value band in the north-west direction in Bazhong increases from 2.5 to 3.0. From the

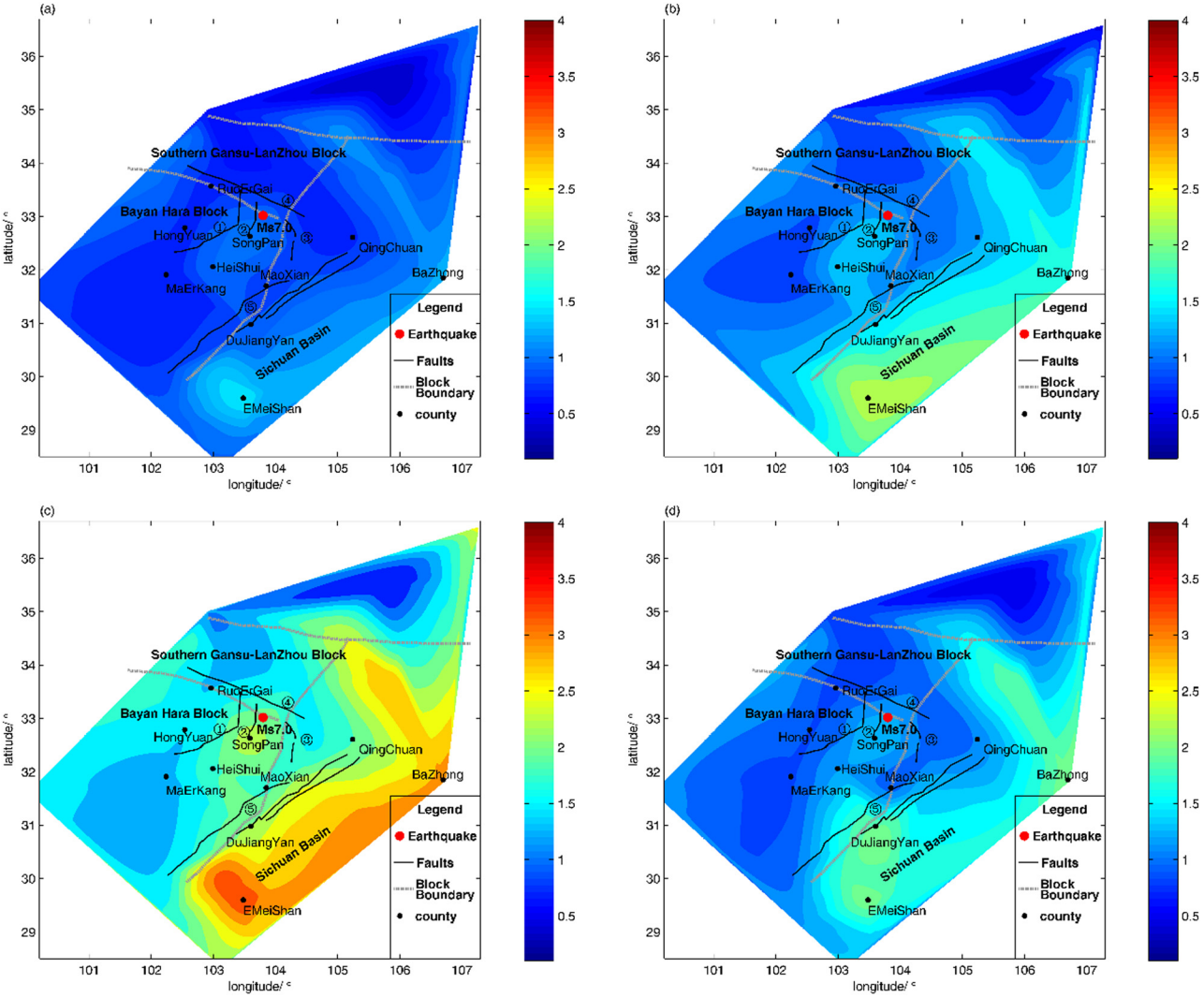

Figure 4: The spatial distribution of the spectral areas. (a) The spatial distribution of the spectral area for May 16–31. (b) The spatial distribution of the spectral area of event 1. (c) The spatial distribution of the spectral area of event 2. (d) The spatial distribution of the spectral area of event 3. The black lines are faults: (1) Longriba Fault, (2) Minjiang Fault, (3) Huya Fault, (4) Tazang Fault, and (5) Longmenshan Fault.

Longmenshan fault zone to the edge of the Sichuan Basin, the value increases gradually. Near Songpan, the value is also higher (2.3–2.5). Figure 4d shows the spatial distribution of event 3. Compared with event 2, the level

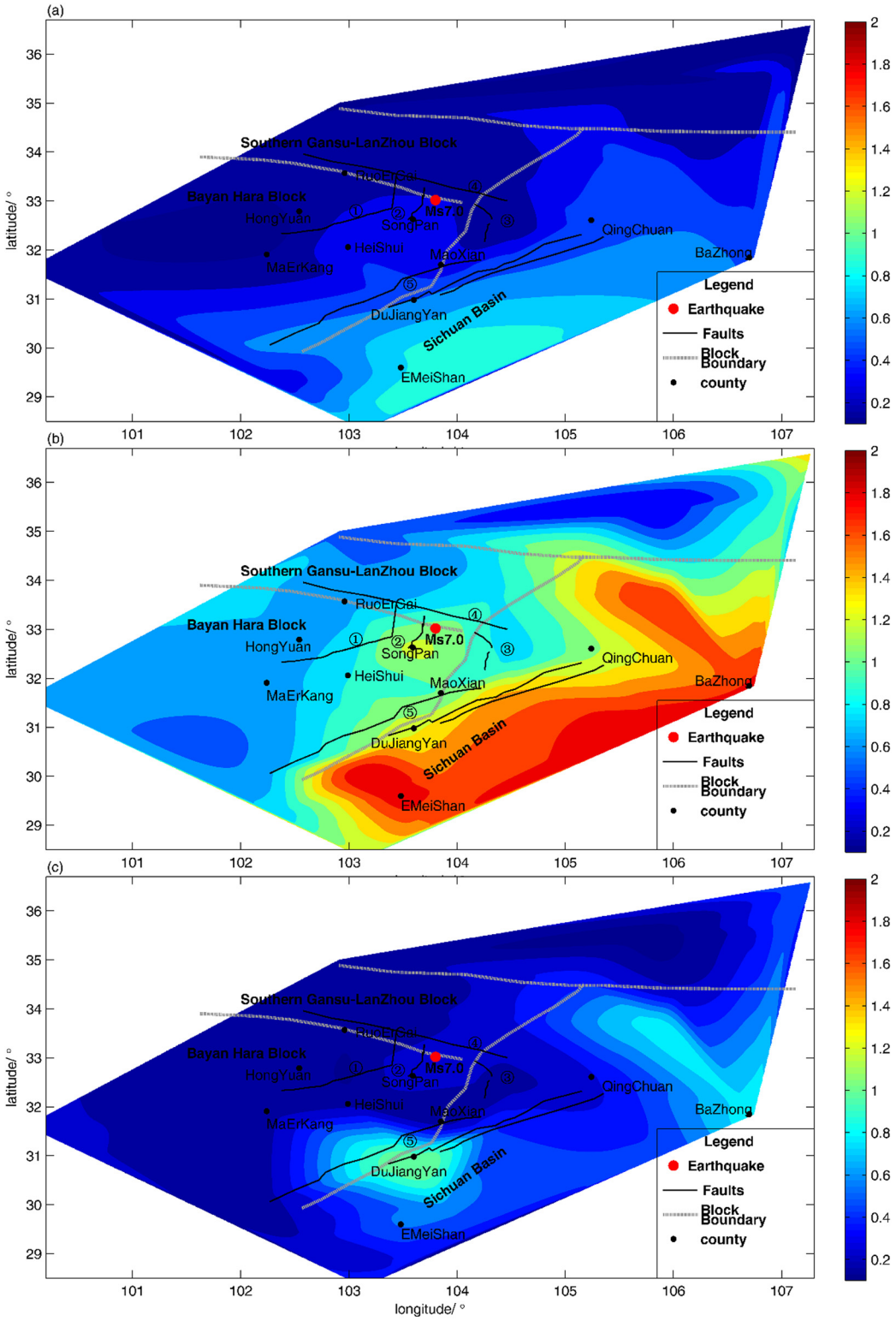

Figure 5: The spatial distribution of the spectral areas denomality. (a) The spatial distribution of the spectral area of event 1. (b) The spatial distribution of the spectral area of event 2. (c) The spatial distribution of the spectral area of event 3. The black lines are faults: (1) Longriba Fault, (2) Minjiang Fault, (3) Huya Fault, (4) Tazang Fault, and (5) Longmenshan Fault.

of event 3 decreases significantly, but it is higher than that of Figure 4a. The high value area is mainly concentrated on both ends of the western margin of the Sichuan Basin. One is in the northwestern part of Bazhong, the other is near Dujiangyan-Emeishan. It seems that the high value area extends northwest. Along the edge of the Sichuan Basin, the value between Bazhong and Emeishan decreases, and the value near Songpan recovers to the same level as that in Figure 4a.

Local geological factors may cause ambient noise local variation, in order to suppress the influence of this difference on the results. Herein, we took the spectral area of May 16–31 as the "normal value," and subtract the normal value from the spectral area of event 1, event 2, and event 3, and the result is shown in Figure 5. Compared with Figures 4 and 5, it can be seen that the distribution region of high value has not changed substantially. It can be considered that the difference of local geological factors has not affected the results of this paper.

The temperatures, pressures, rainfall, and spectral areas of PLT station and TSS station were compared (Figure 6) for PLT stations. The correlation analysis shows that the correlation coefficients of the spectral area and meteorological factors (air temperature, air pressure, and rainfall) are 0.27, 0.24, and 0.16, respectively, for TSS station, they are 0.31, 0.26, and 0.17, respectively. Therefore, there was no obvious correlation between the increase in the spectral area and the meteorological factors in this study.

Several reports point out that the monsoon is a factor of ambient noise variation [8–11]. During this study period, there were the following four typhoons: "MERBOK," "NANMADOL," "TRLAS," and "NORU" (http://www.typhone.org.cn). Herein, we focus on the relationship between NORU and spectral area. NORU is

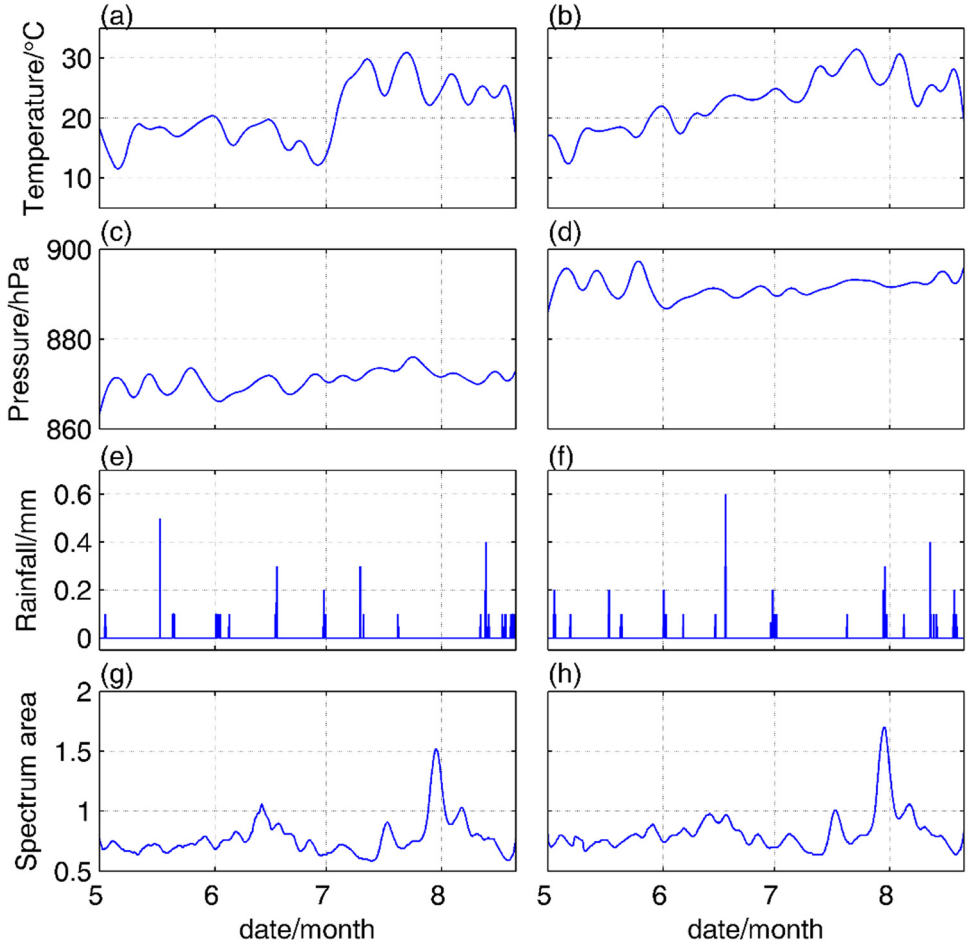

Figure 6: Comparison of the temperatures, pressures, rainfall, and spectral areas of PLT and TSS stations (May 1–August 20, 2017). (a, c, e, and g) Temperatures, pressures, rainfall, and spectral areas of PLT station. (b, d, f, and h) Temperatures, pressures, rainfall, and spectral areas of TSS station.

the strongest typhoon among these typhoons, which occurred from July 19 to August 9, 2017. We show the change in wind speed of NORU and spectral area of SPA and EMS stations in Figure 7. The correlation coefficients of wind speed and spectral area of SPA and EMS are 0.5 and 0.4, respectively. It can be seen that there was little correlation, while the correlation coefficient of the spectral area on two stations is 0.98. In addition, it can be seen that the peak of the spectral area appeared at July 30, whereas the peak of wind speed appeared at July 31. The spectral area recovered on August 2, but the typhoon remained at a high wind speed until August 7. However, we think that the triggering effect of typhoon to earthquake is worth further exploration.

4 Discussion

The spectrum area represents the energy state of the motion. These three events mean that they correspond to the intensification of the three low-frequency ground motions. As for the seismogenic faults of the Ms7.0 Jiuzhaigou earthquake, it is generally accepted that the earthquake occurred on the northward extension of the Huya Fault, which is a left-lateral slip fault [2,12]. The fault plane is nearly upright, and the earthquake has a rupture process extending upward from depth. The Minjiang Fault and the Huya Fault are the main faults on the western and eastern sides, respectively [1–3]. The distribution of the maximum shear strain rate field based on GPS observations in 2013–2016 shows that the southern segment of the Longmenshan Fault was one of the high value areas [5], which coincides with the peak area in Figure 4. Based on the seismographic imaging, magnetotelluric sounding, and aftershock locations, several studies have shown that the movement and physical property difference of the lower and middle crust constitutes the background of the earthquake [12,14]. The Longmenshan Fault system is the intersection of the Qinghai-Tibet block and the South China

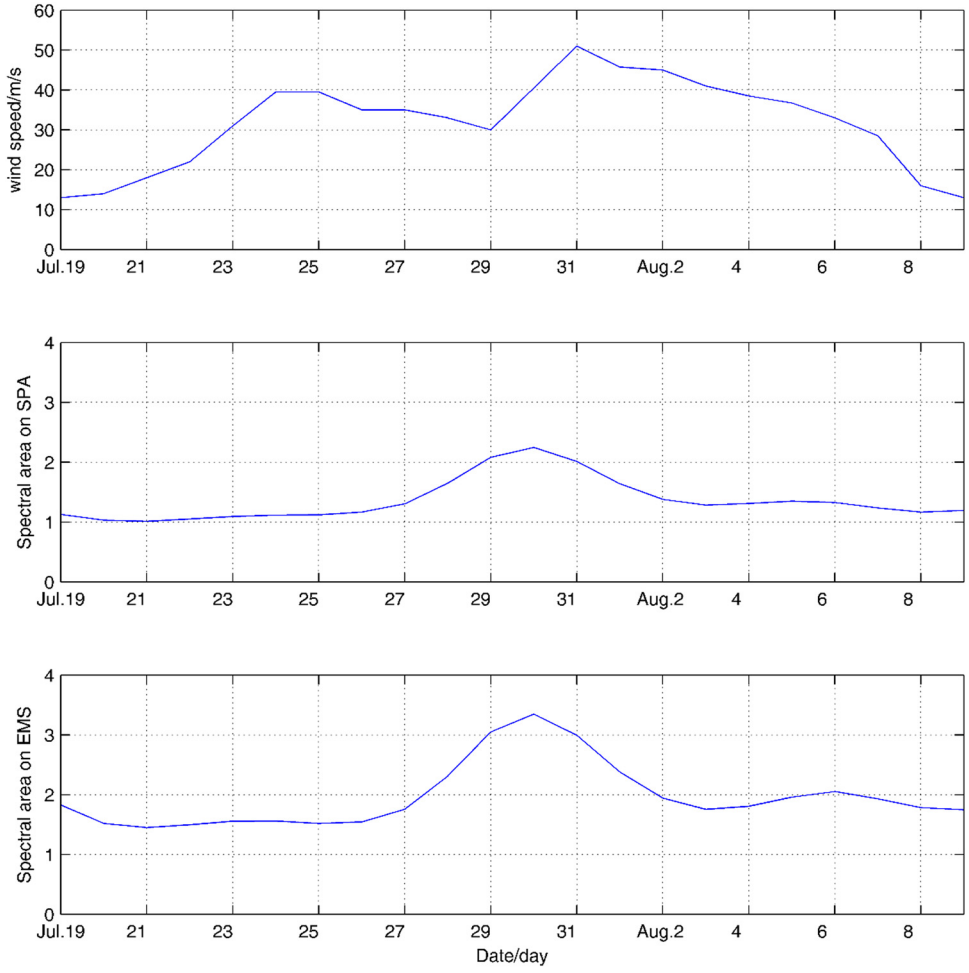

Figure 7: Comparison of the wind speed and spectral areas of SPA and EMS stations.

block. The spatial and temporal characteristics of the three high value ground motion processes that occurred before the earthquake indicate the following. The high values of the ground motion form an approximately U-shaped region in the study area, and the bottom of the U was parallel to the Longmenshan fault zone (Figure 4). We believe that this describes the following process, the eastward movement of the Bayan Hara block, which was obstructed by the rigid crust of the Sichuan Basin. The rheological material in the crust was extruded laterally, the U-shaped area may represent the extrusion process. Based on studies of the crustal flow and dynamic processes in this region, several scholars have pointed out that a diversion phenomenon occurred after the eastward movement of the middle and lower crustal flow was obstructed by the Sichuan Basin [3]. A study of the electrical structure of the region also shows that there is a 10–20 km deep, high conductivity layer between the Minjiang Fault and the Longmenshan Fault, and it shows rheological properties [14]. These are consistent with the results of this study.

Based on the gravity field data, several scholars have studied the 3D density structure and material movement of the Qinghai-Tibetan Plateau using the wavelet multi-scale analysis method. The results show the path and direction of the movement of low-density materials at a depth of 52 km [13]. Near the Emeishan, there was a diverging zone of the lateral extrusion of low-density materials. One branch flowed southward, and the other branch flowed northeastward along the Longmenshan Fault and into the Longmenshan branch again. One branch of the northeastern segment of the faults continues to migrate toward the northeast, whereas the other branch turns to the northwest.

The northeastern side of the U-shaped region (high value area) in Figure 8 is consistent with the location and direction of this low-density zone, which means that the high value area in this study mainly shows the movement of low-density materials within the crust. Therefore, we think that the dynamic background of the Jiuzhaigou earthquake was as follows. First, the eastern movement of the Qinghai-Tibetan block was obstructed by the rigid crust on the eastern side of the Huya Fault, and the energy for the earthquake gathered in the confined areas of the Longriba Fault, the East Kunlun Fault, and the Huya Fault. Second, the eastern movement of the Qinghai-Tibetan block was obstructed in the Sichuan Basin and was diverted (or extruded) at both ends of the Longmenshan Fault, forming a U-shaped movement path.

The results of this study also show that the extrusion at the two ends was not balanced, and the energy at the southwestern end was more concentrated or intense, which exerted an important effect on the enclosed areas

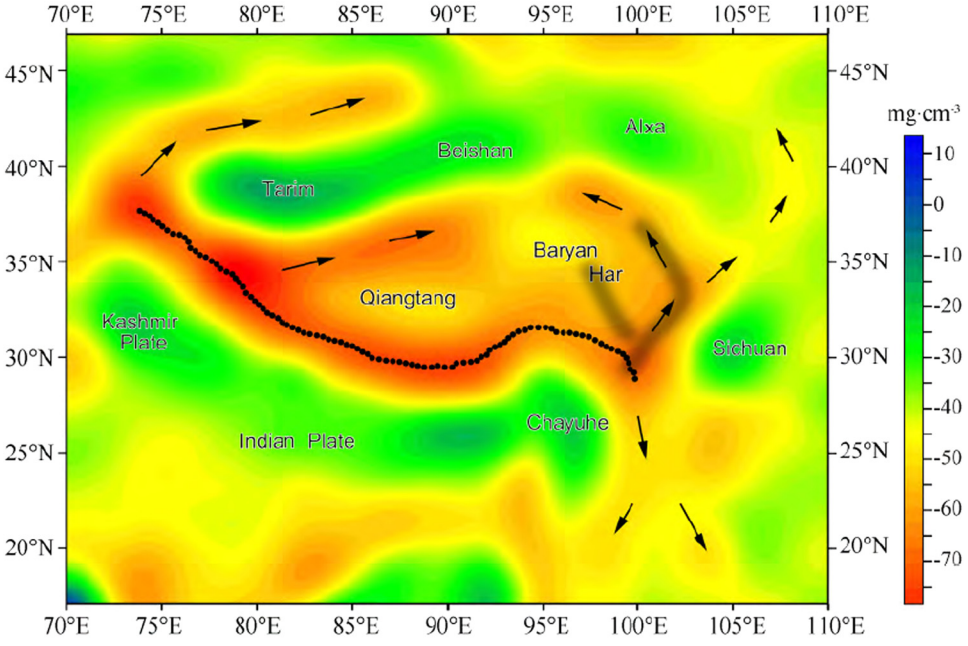

Figure 8: The low-density zones at a depth of 52 km. This figure is from reference [13]. The black arrow indicates the motion direction of the low-density material. The gray area indicates the high value area in this study.

of the Longriba Fault, the East Kunlun Fault, and the Huya fault. The other side of the U-shaped area (northeast) also had an impact on the occurrence of the earthquake, but the southeastern part of the high value area had a more direct role. This is a possible dynamic background for the formation and occurrence of this earthquake. At the very least, we believe that this effect accelerated the occurrence of the Jiuzhaigou earthquake, which coincides with the left-lateral slip mechanism of the earthquake [12].

5 Conclusion

Based on the above discussion, we believe that the high-value process was the reflection of the intense movement of the lower crustal material during the study period, which is related to the Ms7.0 Jiuzhaigou earthquake. These three events show the rapid eastward movement of the lower crustal material. After encountering the obstruction of the Sichuan Basin, the extruded material expanded northwest in the form of a U-shaped high-energy region. These violent movements may be related to the movement of rheological materials in the middle and lower crust. This result is also consistent with the research results of other scholars [1–3,12–14]. We believe that this was the main dynamic factor that caused or triggered the Ms7.0 Jiuzhaigou earthquake.

Acknowledgments: The seismic data were obtained from the Sichuan Seismic Network and the Gansu Seismic Network. Some of the figures were prepared using the Generic Mapping Tools (http://gmt.soest.hawaii.edu/projects/gmt/wiki/Download, last accessed June 2019). The MATLAB code developed by Vaishali Shrivastava was used for some of the calculations (https://ww2.mathworks.cn/matlabcentral/fileexchange/24597-area-under-a-curve, last accessed Sept. 2016). The authors thank LetPub (www.letpub.com) for its linguistic assistance during the preparation of this manuscript. The authors also thank the editors and reviewers for their comments on this manuscript.

Author contributions: YL collected and collated the data. KSX developed the calculated code, performed the calculations, and prepared the manuscript with contributions from co-author.

References

[1] Xu XW, Chen GH, Wang QX, Chen LC, Ren ZK, Xu C, et al. Discussion on seismogenic structure of Jiuzhaigou earthquake and its implication for current straion state in the southeastern Qinghai-Tebet Plateau. Chinese J Geophys. 2017;60(10):4016–8 (in Chinese with English abstract).

[2] Sun J, Yue H, Shen Z, Fang L, Zhan Y, Sun X. The 2017 Jiuzhaigou earthquake: a complicated event occurred in a young fault system. Geophys Res Lett. 2018;45(5):2230–40.

[3] An YR, Su JR, Xue Y, Zhang YY, Bai LS, Liu J, et al. Seismologic characteristics of the 2017 Ms7.0 Jiuzhaigou earthquake, Sichuan, China. Chin Sci Bull. 2018;63(7):663–73 (in Chinese with English abstract).

[4] Zhu JS, Wang XB, Yang YH, Fan J, Cheng XQ. The crustal flow beneath the eastern margin of the Tibetan Plateau and its process of dynamics. Chinese J Geophys. 2017;60(6):2038–57 (in Chinese with English abstract).

[5] Li CT, Su XN, Meng GJ. Heterogeneous strain rate field in the northeast margin of Bayan Har block from GPS observations and its relationship with the 2017 Jiuzhaigou Ms7.0 earthquake. Earthquake. 2018;38(2):37–50 (in Chinese with English abstract).

[6] Li Y, Shao CJ, Li PY, Zhou RJ, Liu YF, Zhang W, et al. Left-lateral strike-slip effect and dynamic mechanism of the Jiuzhaigou Ms 7.0 earthquake in the eastern margin of Tibetan Plateau, China. J Chengdu Univ Technol (Sci Technol Ed). 2017;44(6):641–8 (in Chinese with English abstract).

[7] Shan B, Zheng Y, Liu C, Xie Z, Kong J. Coseismic Coulomb failure stress changes caused by the 2017 M7. 0 Jiuzhaigou earthquake, and its relationship with the 2008 Wenchuan earthquake. Sci China Earth Sci. 2017;60(12):2181–9.

[8] Froment B, Campillo M, Chen JH, Liu QY. Deformation at depth associated with the 12 May 2008 Mw 7.9 Wenchuan earthquake from seismic ambient noise monitoring. Geophys Res Lett. 2013;40(1):78–82.

[9] Obermann A, Froment B, Campillo M, Larose E, Planes T, Valette B, et al. Seismic noise correlations to image structural and mechanical changes associated with the Mw 7.9 2008 Wenchuan earthquake. J Geophys Res Solid Earth. 2014;119(4):3155–68.

[10] Gong M, Shen Y, Li H, Li X, Jia J. Effects of seasonal changes in ambient noise sources on monitoring temporal variations in crustal properties. J Seismol. 2015;19(3):781–90.

[11] Jiang X, Kong X, Guo G. Analysis of seismic anomalies of the Jiuzhaigou earthquake. J Phys Conf Ser. 2019;1187(5):052075.

[12] Xie ZJ, Zheng Y, Yao HJ, Fang LH, Zhang Y, Liu CL, et al. Preliminary analysis on the source properties and seismogenic structure of 2017 Ms7.0 Jiuzhaigou earthquake. Sci China Earth Sci. 2017;48(1):79–92 (in Chinese with English abstract).

[13] Yang WC, Hou ZZ, Yu CQ. Three-dimensional density structure of the Tibetan plateau and crustal mass movement. Chinese J Geophys. 2015;58(11):4223–34 (in Chinese with English abstract).

[14] Zhao GZ, Unsworth MJ, Zhan Y, Wang LF, Chen XB, Jones AG, et al. Crustal structure and rheology of Longmenshan and Wenchuan Mw7.9 earthquake epicentral area from magnetotelluric data. Geology. 2012;40:1139–42.